









Detection of NADH and NADPH levels *in vivo* identifies shift of glucose metabolism in cancer to energy production

Elena V. Potapova¹ , Evgenii A. Zherebtsov² , Valery V. Shupletsov¹ , Viktor V. Dremin^{1,3} , Ksenia Y. Kandurova¹ , Andrian V. Mamoshin^{1,4} , Andrey Y. Abramov^{1,5}  and Andrey V. Dunaev¹ 

1 Research and Development Center of Biomedical Photonics, Orel State University, Russia

2 Optoelectronics and Measurement Techniques Unit, University of Oulu, Finland

3 College of Engineering and Physical Sciences, Aston University, Birmingham, UK

4 Orel Regional Clinical Hospital, Russia

5 Department of Clinical and Movement Neurosciences, UCL Queen Square Institute of Neurology, London, UK

Keywords

energy metabolism; fluorescence lifetime; hepatocellular carcinoma; liver cancer; optical biopsy

Correspondence

E. V. Potapova, Research and Development Center of Biomedical Photonics, Orel State University, 95 Komsomolskaya St, 302026 Orel, Russia

Tel: +79038809438

E-mail: e.potapova@oreluniver.ru

(Received 12 September 2023, revised 15 November 2023, accepted 17 January 2024)

doi:10.1111/febs.17067

Profound changes in the metabolism of cancer cells have been known for almost 100 years, and many aspects of these changes have continued to be actively studied and discussed. Differences in the results of various studies can be explained by the diversity of tumours, which have differing processes of energy metabolism, and by limitations in the methods used. Here, using fluorescence lifetime needle optical biopsy in a hepatocellular carcinoma (HCC) mouse model and patients with HCC, we measured reduced nicotinamide adenine dinucleotide (NADH) and reduced nicotinamide adenine dinucleotide phosphate (NADPH) in control liver, and in HCC tumours and their adjacent regions. We found that NADH level (mostly responsible for energy metabolism) is increased in tumours but also in adjacent regions of the same liver. NADPH level is significantly decreased in the tumours of patients but increased in the HCC mouse model. However, in the *ex vivo* tumour slices of mouse HCC, reactive oxygen species production and glutathione level (both dependent on NADPH) were significantly suppressed. Thus, glucose-dependent NADH and NADPH production in tumours changed but with a more pronounced shift to energy production (NADH), rather than NADPH synthesis for redox balance.

Introduction

Changes in the energy metabolism of tumour cells are now recognised as one of the most important signs of cancer. The most specific metabolic change in malignant cells is the significant increase in glycolytic activity, even in the presence of large amounts of oxygen, known as the Warburg effect [1], although the significance of these metabolic features has been widely discussed. However, numerous studies have confirmed

that cancer cells have multiple genetic mutations that, together with the specific tumour microenvironment, affect various signalling pathways with a strong influence on metabolism. These changes are driven by the essential needs for active growth, proliferation and survival of tumour cells through increased energy production, macromolecular biosynthesis and maintenance of redox balance [2]. It is important to note that

Abbreviations

FS, fluorescence spectroscopy; GSH, glutathione; HCC, hepatocellular carcinoma; HEt, dihydroethidium; MCB, monochlorobimane; NADH, reduced nicotinamide adenine dinucleotide; NADPH, reduced nicotinamide adenine dinucleotide phosphate; PPP, pentose phosphate pathway; ROS, reactive oxygen species.

metabolic adaptation in tumours goes beyond aerobic glycolysis. It has already been shown that cells of the same tumour type developing in the same patient have significantly different levels of glycolysis intensity [3]. Therefore, the use of the glycolysis rate as a sole diagnostic criterion for the detection of malignancy is currently considered to be unreliable. However, the metabolism of glucose in cells is a much more complex process than simple glycolysis and includes other biochemical pathways that are vitally essential for cell homeostasis [2,4]. Thus, the product of glycolysis (pyruvate) is used in the tricarboxylic acid cycle for the production of substrates for respiration and oxidative phosphorylation, including reduced nicotinamide adenine dinucleotide (NADH). Importantly, pyruvate can also be used in lactate dehydrogenase in the cytosol for NADH production [5].

An equally important pathway for glucose utilisation is the pentose phosphate pathway (PPP), which produces pentose phosphates to support increased nucleic acid synthesis and reduced nicotinamide adenine dinucleotide phosphate (NADPH) production [6]. The NADPH cofactor is essential for the biosynthesis of fatty acids and cholesterol, and plays an important role in the production of reduced glutathione (GSH), the major scavenger of reactive oxygen species (ROS), as well as in NO production, and is used by NADPH oxidases [7].

The molecular mechanisms of PPP have been studied extensively in cell lines and tissue slices from animal models of hepatocellular carcinoma (HCC) that can be partially explained by limitations of NADPH measurements in non-homogeneous cell population [8,9]. Increased enzyme activity in the PPP has not been reported in normal hepatocyte proliferation. It is associated with metabolic changes specific to oncological processes.

The two essential metabolic cofactors, NADH and NADPH, are required for energy production and antioxidant defence, respectively, and are generated in distinct pathways of glucose metabolism [10]. Even though both NADPH and NADH can be measured by autofluorescence, these cofactors have a similar spectrum and could not be separated by simple measurement of fluorescence intensity. To date, there have been no studies of metabolic changes in glucose metabolism directly in tissue *in vivo*. However, a new optical system developed at the Research and Development Center of Biomedical Photonics for measuring fluorescence lifetime through a fine-needle probe during percutaneous liver biopsy has suggested that such studies are possible. Time-resolved fluorescence spectroscopy (FS) provides a quantitative distinction between the cofactors NADPH and NADH.

Quantified measurements of the two cofactors by their fluorescence lifetime parameters *in vivo* can become a key approach for gaining a more detailed understanding of cellular metabolism, the way it is changed in malignant tissues *in vivo*, and comparing it to the neighbouring tissue. In this work, we investigate the metabolism in an HCC mouse model and liver of patients with HCC, further extending the methodology proposed by Blacker and Duchon [11] to microscopy to determine the contributions of NADPH and NADH to the total NAD(P)H signal. To assess the level of oxidative stress and the redox status of liver tissue, superoxide anion and reduced GSH were additionally analysed in liver slices immediately after the *in vivo* experiment.

Results

NADH and NADPH levels are increased in the mouse model of HCC

We have previously used a fine needle fibre optic probe to detect and separate the signals of NADH and NADPH, but in contrast to our previous work [12], here we described the results from the actively developing tumour within a short period of its detection, and therefore assumed that we were studying actively proliferating cells.

As a model of the actively developing tumour, the HCC mouse model and control animals were studied using a fine-needle fibre optic probe. Results were obtained with the time-resolved FS channel from a control mouse and two areas in the HCC mouse – from the tumour and adjacent liver (Fig. 1A). Fluorescence signal measurements were processed by the two-exponential fitting model with parameters: τ_1 – short fluorescence lifetime; τ_2 – long fluorescence lifetime; $I_{\alpha 1}$ – the amplitude of the short decay component; $I_{\alpha 2}$ – the amplitude of the long decay component; α_1 – contribution of the short decay component to the total signal; α_2 – contribution of the long decay component to the total signal. Typical χ^2 values obtained from fitting lifetime images to two-component fits are shown in Fig. 1A. All lifetime calculations were fitted to two-components, as determined by obtaining the lowest χ^2 fit value (1.09 ± 0.06 ; 1.14 ± 0.09 , 1.06 ± 0.05 for HCC H33, the adjacent liver tissue and control liver, respectively; Fig. 1B).

Fluorescence intensity values in HCC H33 ($1.7 \times 10^6 \pm 0.6 \times 10^6$ photons) were higher than in the liver tissue of healthy control animals and in liver tissue adjacent to HCC sites ($1.1 \times 10^6 \pm 0.4 \times 10^6$ and $1.3 \times 10^6 \pm 0.7 \times 10^6$ photons, respectively, $P < 0.001$, Fig. 1C). This can be explained by the significant shift

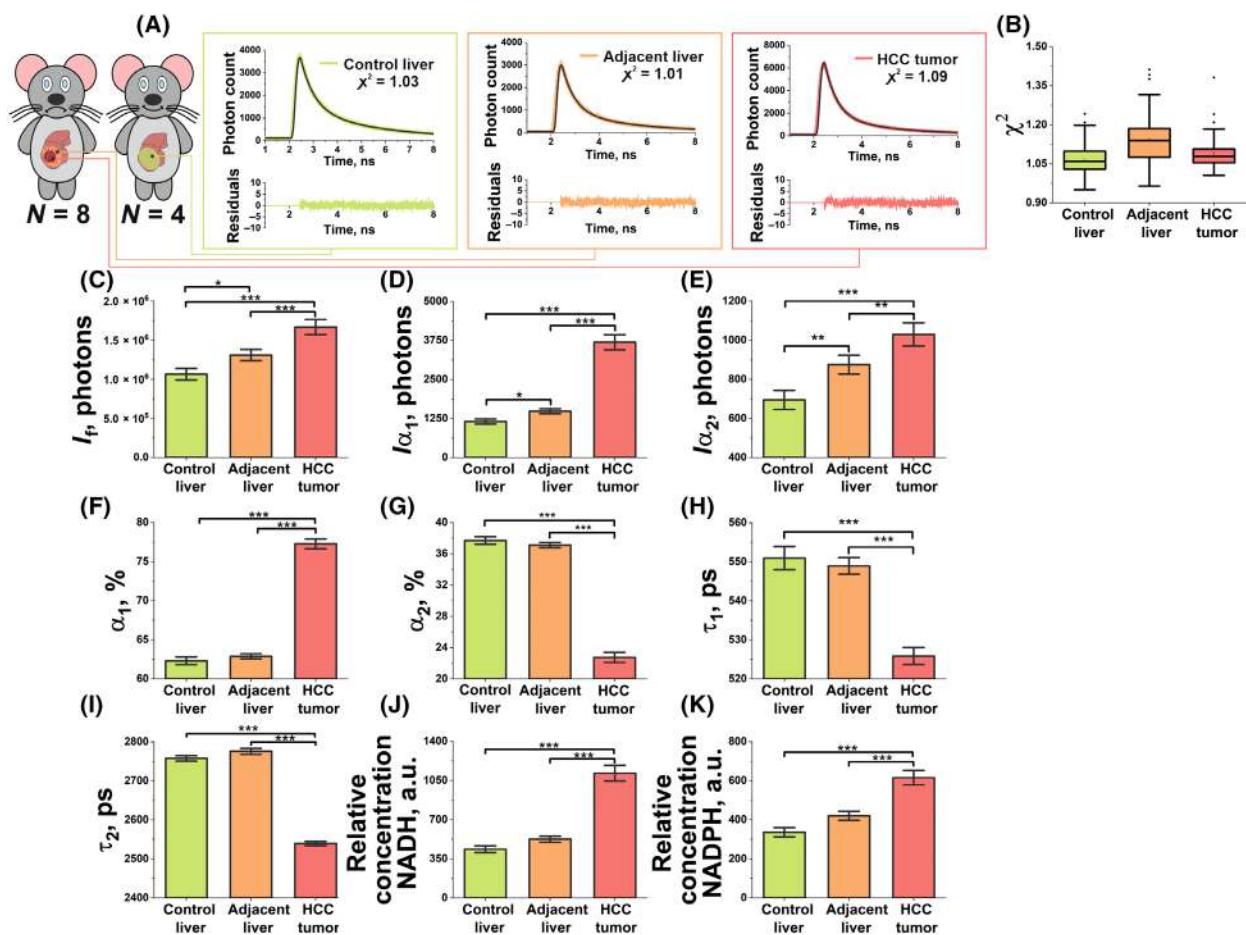


Fig. 1. The parameters calculated by processing the results obtained with the time-resolved FS channel using a fine-needle fibre optic probe in the HCC mouse model and control animals. (A) Scheme of the experiments with typical FS channel recordings; (B) χ^2 fit values; (C) total fluorescence intensity, I_f ; (D) the amplitude of the short decay component, I_{α_1} ; (E) the amplitude of the long decay component, I_{α_2} ; (F) contribution of the short decay component in the total signal, α_1 ; (G) contribution of the long decay component to the total signal, α_2 ; (H) short fluorescence lifetime, τ_1 ; (I) long fluorescence lifetime, τ_2 ; (J) the relative concentrations of NADH; (K) the relative concentrations of NADPH. $N=8$ male mice per group in the HCC mouse model (adjacent liver, $n=202$; HCC tumour, $n=101$). $N=4$ male mice per control group ($n=75$). All data are expressed as mean \pm SEM. The nonparametric Mann–Whitney U -test was chosen to verify the reliability of statistical differences in the results, given the limited sample size. * $P < 0.05$; ** $P < 0.01$; *** $P < 0.001$.

in tumour metabolism, i.e., general accumulation of both NADPH and NADH fluorophores.

The hypothesis of a metabolic shift towards energy metabolism (glycolysis followed by NADH production in tricarboxylic acid cycle) is also supported by the fact that higher fluorescence intensity levels in HCC H33 were associated with a decreased short lifetime component, τ_1 (526 ± 15 ns, Fig. 1H) and its increased contribution, α_1 ($77 \pm 4\%$, Fig. 1F) in the total fluorescence signal relative to these parameters, measured in the liver tissue of healthy control animals τ_1 (551 ± 17 ns, $P < 0.001$, Fig. 1H), α_1 ($62 \pm 3\%$, $P < 0.001$, Fig. 1F) and in liver tissue adjacent to HCC sites τ_1 (549 ± 20 ns, $P < 0.001$, Fig. 1H), α_1 ($63 \pm 3\%$, $P < 0.001$, Fig. 1F). Shorter fluorescence lifetimes correspond to the free form of NADH and

NADPH [13]. It is of particular interest that the fluorescence intensity in liver tissue adjacent to the tumour was also statistically different from that in the liver of control animals ($P < 0.05$), suggesting significant changes in the metabolism of cells in the adjacent liver. The measured parameters of long fluorescence lifetime (τ_2) (Fig. 1I) were also the lowest in HCC H33 (2539 ± 38 ps), while this parameter showed a high level in liver tissue adjacent to HCC sites (2776 ± 74 ps, $P < 0.001$) and the liver tissue of healthy control animals (2758 ± 41 ps, $P < 0.001$). At the same time, it was noted that contribution of the long decay component (α_2) (Fig. 1G) in the total signal in HCC ($23 \pm 4\%$) was significantly lower than in adjacent liver ($37 \pm 3\%$, $P < 0.001$) and control liver ($38 \pm 3\%$, $P < 0.001$).

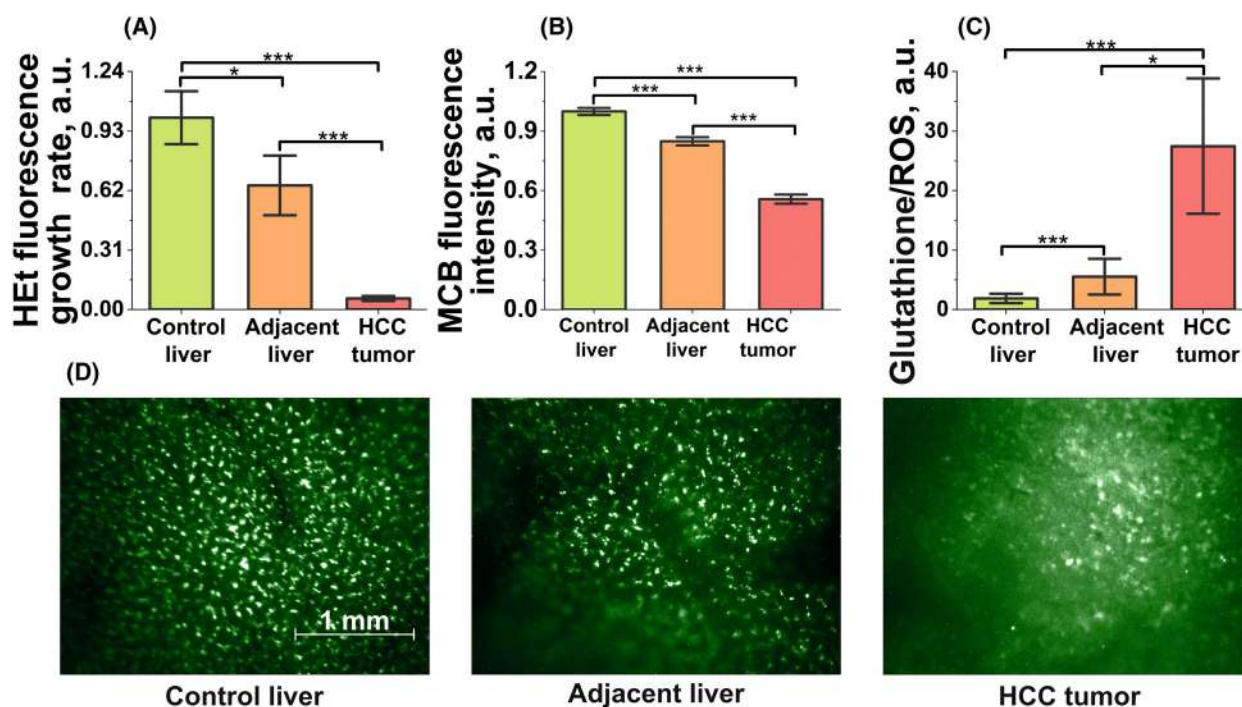


Fig. 2. Changes in the redox balance of HCC tumour and adjacent liver. (A) Rate of ROS production (calculated as the rate of increase of HEt fluorescence, a.u.); (B) level of GSH (MCB fluorescence, a.u.); (C) relative ratio of GSH production to ROS level; (D) representative images (MCB fluorescence). $N=8$ male mice per group in the HCC mouse model (adjacent liver, $n=20$; HCC tumour, $n=20$). $N=4$ male mice per control group ($n=32$). All data are expressed as mean \pm SEM. The nonparametric Mann–Whitney U -test was chosen to verify the reliability of statistical differences in the results, given the limited sample size. Scale bar indicates 1 mm. * $P < 0.05$; *** $P < 0.001$.

We found a significant increase in relative NADH concentration in HCC tumour tissues (1115 ± 464 a.u., $P < 0.001$) compared to the liver tissues of healthy control animals (436 ± 171 a.u., $P < 0.001$) and liver adjacent to HCC sites (526 ± 264 a.u., $P < 0.001$) (Fig. 1J). Calculations of relative NADPH concentration showed a significant increase in NADPH level in adjacent liver and tumour: 615 ± 244 a.u., 336 ± 138 a.u., 420 ± 216 a.u., respectively ($P < 0.001$) in HCC tumour tissues, control liver and liver adjacent to HCC sites (Fig. 1K).

Changes in the redox balance in acute tissue slices of HCC tumour and adjacent liver

The level of NADPH regulates the rate of GSH production in the reaction catalysed by glutathione reductase. The glutathione antioxidant system plays a crucial role in minimising oxidative stress by reacting directly with ROS or by reducing the products of oxidative modification of lipids and proteins. Therefore, after the studies were performed using a fine-needle biopsy device with a time-resolved FS channel, the next step was to assess tissue ROS levels (Fig. 2A) and GSH levels (Fig. 2B) through live cell imaging.

The rate of increase in dihydroethidium (HEt) fluorescence and the level of monochlorobimane (MCB) fluorescence in the healthy liver tissue of control animals were normalised to 1 and all other measurements were adjusted relative to this value. (Note that in the figures it is 1, not 100%.) It was found that the increase in fluorescence of the HEt indicator was significantly lower ($P < 0.001$) in the HCC tumour than in the liver tissue of healthy mice and in the liver adjacent to the tumour: 0.06 ± 0.04 a.u., 1.00 ± 0.52 a.u., 0.65 ± 0.46 a.u., respectively (Fig. 2A). Interestingly, we found that in the HCC tumour, MCB fluorescence showed lower control values 0.56 ± 0.13 compared to 1.00 ± 0.14 and 0.85 ± 0.12 in slices from healthy and tumour-adjacent liver, respectively ($P < 0.001$, Fig. 2B). In order to understand whether the low levels of ROS and GSH in tumour cells actually indicate the absence of oxidative stress in the tissues, we proposed to assess the ratio of GSH production to the level of ROS (Fig. 2C). We found that the endogenous antioxidant content in HCC tissues is significantly higher than the production of ROS, which may indirectly support the findings of increased relative concentration of NADPH described above. Representative confocal images of MCB from the healthy liver tissue of control

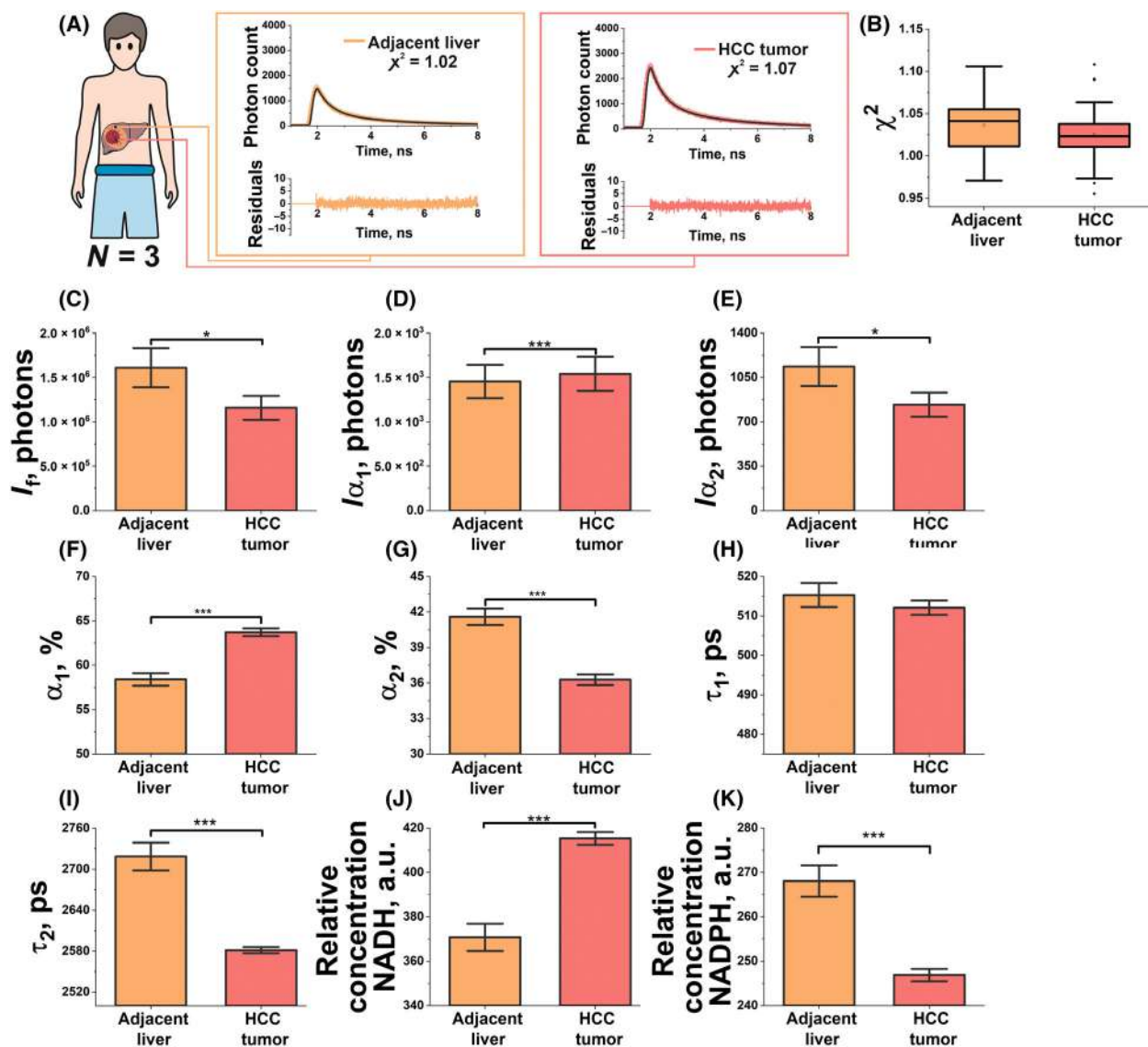


Fig. 3. The parameters calculated by processing the results obtained with the time-resolved FS channel using a fine-needle fibre optic probe in cancer and liver tissue. (A) Scheme of the experiments with typical FS channel recordings; (B) χ^2 fit values; (C) total fluorescence intensity, I_f ; (D) the amplitude of the short decay component, I_{α_1} ; (E) the amplitude of the long decay component, I_{α_2} ; (F) contribution of the short decay component to the total signal, α_1 ; (G) contribution of the long decay component to the total signal, α_2 ; (H) short fluorescence lifetime, τ_1 ; (I) long fluorescence lifetime, τ_2 ; (J) the relative concentrations of NADH; (K) the relative concentrations of NADPH. $N=3$ (two female and one male) patients (adjacent liver, $n=47$; HCC tumour, $n=59$). All data are expressed as mean \pm SEM. The nonparametric Mann–Whitney U -test was chosen to verify the reliability of statistical differences in the results, given the limited sample size. * $P < 0.05$; *** $P < 0.001$.

animals, tumour-adjacent liver and tumour are presented in Fig. 2D.

Clinical studies indicate increased NADH but decreased NADPH level in HCC tumour

Percutaneous needle biopsy was performed on a scheduled basis in patients with suspected liver malignancy.

In each patient, the fluorescence signals were recorded in liver tissue adjacent to the tumour along the movement of the puncture needle and directly in the tumour itself. Figure 3 shows the results of the time-resolved FS for clinical studies. Typical χ^2 values obtained from fitting lifetime images to two-component fits are shown in Fig. 3A. All lifetime calculations were fitted to two-components, as determined by obtaining the lowest χ^2

fit value (1.03 ± 0.03 ; 1.04 ± 0.03 for tumour HCC and the adjacent liver tissue, respectively; Fig. 3B).

We found that measurements of human HCC had some similarity to mouse HCC H33 calculated parameters. Thus, there was an increase in the intensity and contribution of the first component, α_1 , to the total signal in tumour compared to liver ($64 \pm 2\%$ vs. $58 \pm 3\%$, $P < 0.001$, Fig. 3F). However, the duration of the short decay component, τ_1 , tended to decrease in tumour tissue compared to liver (512 ± 9 ps vs. 516 ± 14 ps, $P < 0.001$, Fig. 3H). At the same time, we found a significant decrease in the long fluorescence lifetime, τ_2 in cancer compared to liver tissue (2681 ± 24 ps vs. 2719 ± 93 ps, $P < 0.001$, Fig. 3I) and reduction in the contribution of this component to the total signal in tumour compared to liver ($36 \pm 2\%$ vs. $42 \pm 3\%$, $P < 0.001$, Fig. 3G). In agreement with our previous study, we found a significant contribution of NADH in the signal generation in the tumour [12]. All this supports the hypothesis of a metabolic shift towards energy metabolism (including glycolysis).

The parameter τ_2 is closest in human HCC and murine HCC H33. Thus, we recorded values in the tumour that were significantly lower than in the surrounding liver tumour: 2581 ± 24 ps vs. 2719 ± 14 ps, $P < 0.001$ (Figs 1I and 3I). We also found that the relative concentration of coenzyme NADPH in the tumour was significantly decreased compared to the surrounding tissue: 246 ± 12 a.u. vs. 268 ± 30 a.u., $P < 0.001$ (Fig. 3K).

Discussion

As mentioned above, the glycolytic pathway and the PPP are two metabolic pathways that are closely linked and regulate glucose uptake together. In cancer, energy metabolism is significantly altered, providing many benefits to tumour cells, including stimulation of biosynthesis, ATP production, detoxification and support for rapid proliferation [14].

To prevent excessive oxidative stress, tumour cells regulate the production of antioxidant enzymes and extensively use their metabolic pathways to ensure an adequate supply of antioxidant molecules (such as GSH and NADPH). Some of the energy substrates involved in these pathways can also be redirected to specific pathways that produce not only antioxidant molecules (NADPH and GSH) but also redox cofactors (including NADH) that are used to maintain or restore adequate redox homeostasis.

Under hypoxia, cells prioritise glycolysis over oxidative phosphorylation for ATP production. Therefore, the decrease in the short lifetime component τ_1 and

the increase its fraction α_1 measured *in vivo* in tumour tissues is consistent with the increased levels of glycolysis expected in malignant tissues [15]. The hypothesis of a glycolytic pathway in the tumour is supported by temporally resolved FS results in both preclinical studies in laboratory mice and percutaneous liver biopsies in the clinic.

Pentose phosphate pathway is a major component of cellular metabolism that is critical for cancer cells. Potentially the most valuable function of PPP in carcinogenesis is the protection against cell death. It is essential to control ROS generated by accelerated metabolism, hypoxia or DNA damage, to maintain a high proliferative advantage of cancer cells in the tumour environment. Oxidative activation of PPP may help transformed cells to avoid oxidative stress by increasing the intracellular redox capacity of cancer cells through enhanced NADPH production. In our study, in the murine model we demonstrated an increase in NADPH cofactor production in tumour cells relative to surrounding tissue using an *in vivo* optical biopsy approach we had developed. Our findings are consistent with evidence that increased NADPH production reduces intracellular ROS levels in HCC [16]. The activation of the Akt pathway, a common genetic alteration in HCC, can influence glucose metabolism and potentially impact NADH and NADPH levels. Akt activation promotes glucose uptake and glycolysis, which can lead to increased NADH production. Moreover, Akt signalling may enhance the PPP activity, which generates NADPH [17]. Similar to that, loss of p53 function, another genetic alteration observed in HCC, also affects cellular metabolism and redox balance. The antitumour protein is involved in regulating glycolysis and oxidative phosphorylation. Its inactivation leads to enhanced glycolysis, potentially increasing NADH levels. Additionally, p53 influences the expression of genes involved in NADPH generation, such as G6PD, which could impact NADPH levels [18].

It is worth noting that a particularly interesting part of the work was the comparison of the *in vivo* data with the results of an *in vitro* oxidative stress study. The fluorescent probe HET was used to study ROS levels. Although it can interact with different free radicals and cannot be used as a specific indicator of specific forms of ROS, it is mainly oxidised by the superoxide anion [19]. As an antioxidant, GSH is an important component in maintaining the normal redox state of cells, helping to prevent or reverse oxidative modifications that lead to mitochondrial dysfunction and cell death. The importance of GSH lies not only in its quantity but also in the versatility of its chemical

interaction with different types of ROS [2]. We have found that the antioxidant defence in tumour tissue is highly efficient and significantly exceeds ROS levels. This may support evidence for an essential role for PPP in tumour metabolism and is consistent with our *in vivo* time-resolved FS data showing that NADPH levels are significantly higher in tumours than in surrounding tissues.

It should be emphasised that, based on the data on the relative concentrations of NADH and NADPH cofactors, the majority of the glucose metabolic pathway is most likely oriented towards maintaining the energy balance of the cell in a glycolytic way. The data from the PPP study are not very conclusive at this stage. We associate the resulting differences in the relative concentration of NADPH with a small sample of individuals or with a different metabolic organisation in the actual tumour. It is possible that the development of relatively aggressive primary liver tumours may be associated with a decrease in antioxidant defences. The technology proposed in this paper to assess NADH and NADPH cofactor levels for the first time provides direct information during surgery and may help researchers and clinicians to understand the underlying processes of glucose utilisation, which will allow adjustments to treatment and the development of new pharmacological therapies for cancer.

Conclusion

High energy demands and an abnormal tumour micro-environment induce changes in cancer metabolism. Tumour cells rearrange their metabolism and rely on high rates of aerobic glycolysis to meet their additional needs for growth and survival. In addition, metabolic stress inevitably induces ROS-mediated oxidative stress, even under conditions of hypoxia, making NADPH homeostasis critical for cell survival.

The ability to study the metabolic shift in tumour cells *in vivo* offers a great opportunity for both diagnosis and further treatment strategies for patients, as well as therapeutic strategies for cancer treatment. Future work will focus on analysing clinical data and looking for correlations between PPP activation, the type of liver tumour (primary or metastatic) and its aggressiveness.

Materials and methods

Fluorescence intensity and lifetime measurements

In vivo fluorescence intensity and lifetime measurements of liver cancer metabolic changes in NAD(P)H levels were

performed using our fluorescence lifetime system, custom designed for optical percutaneous needle biopsy of the liver, which has been previously described [10]. Briefly, excitation was provided by a pulsed BDL-SMN 375 nm UV laser (Becker & Hickl GmbH, Berlin, Germany; 80 MHz repetition rate, 40 ps pulse width). Emission light was separated using a band-pass filter and detected with an HPM-100-40 hybrid photomultiplier tube (Becker & Hickl GmbH) with high quantum efficiency and minimal afterpulsing. Data acquisition was performed using time-correlated single photon counting hardware (SPC-130-EMN; Becker & Hickl GmbH) and control software (SPCM; Becker & Hickl GmbH). The measurement channel was incorporated into the optical needle probe of 1 mm in diameter, compatible with the standard equipment for the puncture biopsy procedure [20].

To measure the total ROS production and the level of reduced GSH in acute liver slices, we used a custom fluorescence microscopy setup. M455F1 LED (Thorlabs Inc., Newton, NJ, USA) and BDL-SMN-375 UV laser were used to excite the fluorescence of HEt (Invitrogen, Carlsbad, CA, USA) oxidation products and the conjugation product in the reaction between MCB (Invitrogen) and GSH, respectively. To avoid the accumulation of oxidised products, HEt was not pre-loaded to the slices but was added at the beginning and was present in the chamber during the experiments (5 μ M). For GSH measurements, the slices were preloaded with 50 μ M MCB solution. MCB measurements were averaged in five images per slice.

Animal studies

The experimental liver tumour model was a hybrid mouse namely the B6D2F1 (BDF1) mouse ((C57BL/6 \times DBA/2) F1) inoculated by injection of a suspension of H33 mouse HCC cells into the right medial lobe of the liver. The H33 murine model of HCC is a genetically engineered mouse model used in liver cancer research. It is designed to recapitulate key genetic alterations observed in human HCC, such as activation of the Akt pathway, inactivation of p53, activation of β -catenin and overexpression of c-Myc [21]. The experimental studies were performed in accordance with the Principles of Good Laboratory Practice (GLP). The work was approved by the Ethics Committee of Orel State University (licence number 12 of 06.09.2018). BDF1 three-month-old mice, comprising eight male mice with early-stage HCC tumours and four healthy male control animals, were used in the experiments. These mice were provided by the N.N. Blokhin Cancer Research Center (Moscow, Russia) [22]. The tumour seeding procedure was developed and certified by this research centre. Mice were housed under controlled environmental conditions (20–26 °C, 30–70% relative humidity). The animals were fed *ad libitum* with a balanced granulated diet according to their daily physiological requirements.

Studies were carried out as soon as an animal developed the first signs of a tumour. Body weight, abdominal

circumference, presence of ascites, anterior abdominal wall muscle tension, palpation of a tumour-like mass, decreased appetite and motor activity were assessed in the mice. The animals were first anaesthetised by intramuscular injection of Zoletil 100 (Vibrac, Carros, France) and Xyla (Interchemie, Venray, the Netherlands) at standard doses. Each mouse was fixed in the supine position on a special platform. The Rodent Surgical Monitor+ (Indus Instruments, Webster, TX, USA) was used to monitor the physiological state of the mouse during the measurements. After induction of deep anaesthesia, a laparotomy was performed to gain access to the abdominal cavity and to perform the *in vivo* optical measurements in liver tissue and tumours. In addition to *in vivo* measurements, ROS production and the level of reduced GSH in acute liver slices were studied. The liver was extracted and removed into a cold Hanks' Balanced Salt Solution (pH 7.4/4 °C), with subsequent slices performed at a thickness of 300–500 µm.

***In vivo* clinical studies**

Preliminary, clinical measurements were performed at the department of interventional radiology of Orel Regional Clinical Hospital (Orel, Russia). The study was approved by the Ethics committee of Orel State University (licence number 14 of 24.01.2019) and carried out in accordance with the 2013 Declaration of Helsinki by the World Medical Association. Three (two female and one male) patients diagnosed with HCC participated in the clinical trials. All of the patients signed an informed consent form prior to the study.

Measurements in the murine model and in HCC patients were supported and confirmed by histological analysis.

Data analysis

Histograms represent the mean and standard error of the mean. The nonparametric Mann–Whitney *U*-test was chosen to verify the reliability of statistical differences in the results, given the limited sample size. A *P*-value < 0.05 was considered statistically significant for either test.

The proportions of NADH and NADPH cofactors in the total NAD(P)H signal were calculated using the approach described in [11] using the formulas:

$$[\text{NADH}]_{\text{bound}} = k \left(\frac{4.4 - \tau_{\text{bound}}(\text{ns})}{2.9} \right) \frac{I_{\text{total}}}{(1 - \alpha_{\text{bound}})\tau_{\text{free}} + \alpha_{\text{bound}}\tau_{\text{bound}}}, \quad (1)$$

$$[\text{NADPH}]_{\text{bound}} = k \left(\frac{\tau_{\text{bound}}(\text{ns}) - 1.5}{2.9} \right) \frac{I_{\text{total}}}{(1 - \alpha_{\text{bound}})\tau_{\text{free}} + \alpha_{\text{bound}}\tau_{\text{bound}}}, \quad (2)$$

where *k* is an arbitrary constant related to the variables describing the experimental system [23]. We assumed *k* = 1 in our calculations and performed a semi-quantitative analysis of the relative concentrations of NADH and NADPH.

Acknowledgements

The authors are very grateful to Dr Olga V. Morozova (N.N. Blokhin Russian Cancer Research Center, Moscow, Russia) for tumour cell inoculation. The authors acknowledge the support of the Russian Science Foundation under project no. 21-15-00325 (development of an optical biopsy system and conducting experimental study) and the grant of the Russian Federation Government no. 075-15-2022-1095 (separation and analysis of NADH and NADPH).

Conflict of interest

The authors declare no conflict of interest.

Author contributions

EVP, AVM, AYA, and AVD contributed to the conceptualisation and design of methodology. VVS, KYK, and AVM contributed to the investigation and data curation. VVS, VVD, EAZ, and KYK contributed to the formal analysis and visualisation. EVP, EAZ, VVD, and AYA contributed to the writing—original draft preparation. EVP, EAZ, VVD, KYK, VVS, AVM, AYA, and AVD contributed to the writing—review and editing. EVP, AYA, and AVD contributed to the project administration. AYA and AVD contributed to the supervision and funding acquisition.

Data availability statement

Data underlying the results may be obtained from the authors upon reasonable request.

References

- 1 Warburg O, Wind F & Negelein E (1926) Ueber den stoffwechsel von tumoren im körper. *Klin Wochenschr* **5**, 829–832.
- 2 Cairns RA, Harris IS & Mak TW (2011) Regulation of cancer cell metabolism. *Nat Rev Cancer* **11**, 85–95.
- 3 Woitek R & Gallagher FA (2021) The use of hyperpolarised ¹³C-MRI in clinical body imaging to probe cancer metabolism. *Br J Cancer* **124**, 1187–1198.
- 4 Gupta S, Roy A & Dwarakanath BS (2017) Metabolic cooperation and competition in the tumor microenvironment: implications for therapy. *Front Oncol* **7**, 68.
- 5 Stryer L, Berg JM, Tymoczko JL & Gatto GJ (2019) *Biochemistry*. W. H. Freeman, New York, NY.
- 6 Mayes PA & Bender DA (2003) The pentose phosphate pathway & other pathways of hexose metabolism. In

- Harper's Illustrated Biochemistry (Murray RK, Granner DK, Mayes PA & Rodwell VW, eds), pp. 163–172. Lange Medical Books/McGraw-Hill, New York, NY.
- 7 Aquilano K, Baldelli S & Ciriolo MR (2014) Glutathione: new roles in redox signaling for an old antioxidant. *Front Pharmacol* **5**, 196.
 - 8 Kowalik MA, Columbano A & Perra A (2017) Emerging role of the pentose phosphate pathway in hepatocellular carcinoma. *Front Oncol* **7**, 87.
 - 9 Kowalik MA, Guzzo G, Morandi A, Perra A, Menegon S, Masgras I, Trevisan E, Angioni MM, Fornari F & Quagliata L (2016) Metabolic reprogramming identifies the most aggressive lesions at early phases of hepatic carcinogenesis. *Oncotarget* **7**, 32375–32393.
 - 10 Esteras N, Blacker TS, Zherebtsov EA, Stelmashuk OA, Zhang Y, Wigley WC, Duchen MR, Dinkova-Kostova AT & Abramov AY (2023) Nrf2 regulates glucose uptake and metabolism in neurons and astrocytes. *Redox Biol* **62**, 102672.
 - 11 Blacker TS & Duchen MR (2016) Investigating mitochondrial redox state using NADH and NADPH autofluorescence. *Free Radic Biol Med* **100**, 53–65.
 - 12 Zherebtsov EA, Zherebtsov EA, Zherebtsov EA, Zherebtsov EA, Potapova EV, Potapova EV, Potapova EV, Mamoshin AV, Mamoshin AV, Shupletsov VV *et al.* (2022) Fluorescence lifetime needle optical biopsy discriminates hepatocellular carcinoma. *Biomed Opt Express* **13**, 633–646.
 - 13 Blacker TS, Marsh RJ, Duchen MR & Bain AJ (2013) Activated barrier crossing dynamics in the non-radiative decay of NADH and NADPH. *Chem Phys* **422**, 184–194.
 - 14 Jiang P, Du W & Wu M (2014) Regulation of the pentose phosphate pathway in cancer. *Protein Cell* **5**, 592–602.
 - 15 Skala MC, Riching KM, Bird DK, Gendron-Fitzpatrick A, Eickhoff J, Eliceiri KW, Keely PJ & Ramanujam N (2007) *In vivo* multiphoton fluorescence lifetime imaging of protein-bound and free NADH in normal and pre-cancerous epithelia. *J Biomed Opt* **12**, 24014.
 - 16 Jin L & Zhou Y (2019) Crucial role of the pentose phosphate pathway in malignant tumors. *Oncol Lett* **17**, 4213–4221.
 - 17 Hoxhaj G, Ben-Sahra I, Lockwood SE, Timson RC, Byles V, Henning GT, Gao P, Selfors LM, Asara JM & Manning BD (2019) Direct stimulation of NADP+ synthesis through Akt-mediated phosphorylation of NAD kinase. *Science* **363**, 1088–1092.
 - 18 Jiang P, Du W, Wang X, Mancuso A, Gao X, Wu M & Yang X (2011) p53 regulates biosynthesis through direct inactivation of glucose-6-phosphate dehydrogenase. *Nat Cell Biol* **13**, 310–316.
 - 19 Zhao H, Kalivendi S, Zhang H, Joseph J, Nithipatikom K, Vásquez-Vivar J & Kalyanaraman B (2003) Superoxide reacts with hydroethidine but forms a fluorescent product that is distinctly different from ethidium: potential implications in intracellular fluorescence detection of superoxide. *Free Radic Biol Med* **34**, 1359–1368.
 - 20 Dremin V, Potapova E, Zherebtsov E, Kandurova K, Shupletsov V, Alekseyev A, Mamoshin A & Dunaev A (2020) Optical percutaneous needle biopsy of the liver: a pilot animal and clinical study. *Sci Rep* **10**, 1–11.
 - 21 Brown ZJ, Heinrich B & Greten TF (2018) Mouse models of hepatocellular carcinoma: an overview and highlights for immunotherapy research. *Nat Rev Gastroenterol Hepatol* **15**, 536–554.
 - 22 Lazarevich NL, Cheremnova OA, Varga EV, Ovchinnikov DA, Kudrjavitseva EI, Morozova OV, Fleishman DI, Engelhardt NV & Duncan SA (2004) Progression of HCC in mice is associated with a downregulation in the expression of hepatocyte nuclear factors. *Hepatology* **39**, 1038–1047.
 - 23 Xu C & Webb WW (1996) Measurement of two-photon excitation cross sections of molecular fluorophores with data from 690 to 1050 nm. *J Opt Soc Am B* **13**, 481–491.